

---

# Airway Pressure Release Ventilation Reduces Conducting Airway Micro-Strain in Lung Injury



Michaela Kollisch-Singule, MD, Bryanna Emr, MD, Bradford Smith, PhD, Cynthia Ruiz, Shreyas Roy, MD, Qinghe Meng, MD, Sumet Jain, MD, Joshua Satalin, BS, Kathy Snyder, Auyon Ghosh, MD, William H Marx, DO, FACS, Penny Andrews, RN, Nader Habashi, MD, Gary F Nieman, BA, Louis A Gatto, PhD

---

**BACKGROUND:** Improper mechanical ventilation can exacerbate acute lung damage, causing a secondary ventilator-induced lung injury (VILI). We hypothesized that VILI can be reduced by modifying specific components of the ventilation waveform (mechanical breath), and we studied the impact of airway pressure release ventilation (APRV) and controlled mandatory ventilation (CMV) on the lung micro-anatomy (alveoli and conducting airways). The distribution of gas during inspiration and expiration and the strain generated during mechanical ventilation in the micro-anatomy (micro-strain) were calculated.

**STUDY DESIGN:** Rats were anesthetized, surgically prepared, and randomized into 1 uninjured control group ( $n = 2$ ) and 4 groups with lung injury: APRV 75% ( $n = 2$ ), time at expiration ( $T_{Low}$ ) set to terminate appropriately at 75% of peak expiratory flow rate (PEFR); APRV 10% ( $n = 2$ ),  $T_{Low}$  set to terminate inappropriately at 10% of PEFR; CMV with PEEP 5 cm H<sub>2</sub>O (PEEP 5;  $n = 2$ ); or PEEP 16 cm H<sub>2</sub>O (PEEP 16;  $n = 2$ ). Lung injury was induced in the experimental groups by Tween lavage and ventilated with their respective settings. Lungs were fixed at peak inspiration and end expiration for standard histology. Conducting airway and alveolar air space areas were quantified and conducting airway micro-strain was calculated.

**RESULTS:** All lung injury groups redistributed inspired gas away from alveoli into the conducting airways. The APRV 75% minimized gas redistribution and micro-strain in the conducting airways and provided the alveolar air space occupancy most similar to control at both inspiration and expiration.

**CONCLUSIONS:** In an injured lung, APRV 75% maintained micro-anatomic gas distribution similar to that of the normal lung. The lung protection demonstrated in previous studies using APRV 75% may be due to a more homogeneous distribution of gas at the micro-anatomic level as well as a reduction in conducting airway micro-strain. (J Am Coll Surg 2014;219:968–976. © 2014 by the American College of Surgeons)

---

**Disclosure Information:** Nothing to disclose.

Support: This work was supported by an AMA Foundation Seed Grant and NIH grant R21 HL092801. The Foundation took no part in the design and conduct of the study, collection, management, analysis, or interpretation of the data.

Presented at American College of Surgeons Committee on Trauma Resident National (March 2014), Upstate NY (November 2013), and Region 2 (December 2013) competitions and awarded First Place for Basic Laboratory Science.

Received June 12, 2014; Revised July 25, 2014; Accepted August 1, 2014. From the Department of General Surgery, SUNY Upstate Medical University, Syracuse, NY (Kollisch-Singule, Emr, Roy, Meng, Jain, Satalin, Snyder, Ghosh, Marx, Nieman, Gatto); the Department of Medicine, University of Vermont, Burlington, VT (Smith); Department of Biological Sciences, SUNY Cortland, Cortland, NY (Ruiz, Gatto); and the R Adams Cowley Shock Trauma Center, Trauma Critical Care Medicine, University of Maryland School of Medicine, Baltimore, MD (Andrews, Habashi). Correspondence address: Joshua Satalin, BS, SUNY Upstate Medical University, 750 E Adams St, Syracuse, NY 13210. email: [satalinj@upstate.edu](mailto:satalinj@upstate.edu)

In patients with lung injury, mechanical ventilation is a necessary, life-saving treatment. However, improper mechanical ventilation settings can induce or exacerbate lung injury by causing a secondary ventilator-induced lung injury (VILI).<sup>1</sup> Several mechanisms of VILI have been described, including atelectrauma, which is caused by the large pressure gradients<sup>2,3</sup> present during the reopening (recruitment) of closed airways and alveoli, as well as volutrauma, which is a consequence of parenchymal overdistension.<sup>4</sup> Despite implementation of ventilation strategies to protect against these damaging stimuli, mortality from adult respiratory distress syndrome remains unacceptably high.<sup>5,6</sup> Whole lung stress and strain have been used to identify the pathologic impact of a

**Abbreviations and Acronyms**

$A_a$	= alveolar area
APRV	= airway pressure release ventilation
$C_a$	= conducting airway air space area
CMV	= controlled mandatory ventilation
PEFR	= peak expiratory flow rate
$T_{Low}$	= time during expiratory release
T-PEFR	= termination of peak expiratory flow rate
VILI	= ventilator induced lung injury
$V_t$	= tidal volume

given mechanical ventilation pattern (mechanical breath) on the entire lung. Whole lung macro-strain is elevated in humans with lung injury,<sup>7</sup> and it has been suggested that dynamic strain is more injurious than static.<sup>8</sup> However, because of lung heterogeneity, macro-strain may not describe the substantial regional stress and strain heterogeneity in the distal air space, so the concept of regional micro-strain has recently been described.<sup>9</sup>

Historically, study of the dynamic relationship between alveoli and conducting airways has been inhibited by the complex geometry of this micro-anatomic network.<sup>10</sup> Therefore, the intricacies of dynamic micromechanics have not been fully elucidated.<sup>11</sup> Alveolar micro-strain was recently characterized in the injured lung using in vivo microscopy of subpleural alveoli.<sup>9</sup> This study explored the effect of altering the timing and magnitude of the applied ventilation pressures on alveolar micro-strain and recruitment, demonstrating the importance of studying the impact of the mechanical breath at the micro-anatomic level.

Although in vivo microscopy provides a direct and dynamic view of alveolar mechanics, the analysis is limited to the subpleural alveoli and does not characterize the space-occupying relationship between the alveoli and conducting airways.<sup>9</sup> In order to study the impact of varying mechanical breaths on the conducting airways, we use a novel histologic analysis of the terminal airway (ie, alveoli and conducting airways), which allows quantification of conducting airway micro-strain.<sup>12</sup> Understanding the impact of specific components of the mechanical breath, such as the inspiratory pressure and the time at end expiration at the micro-anatomic level, is important to the development of optimal protective ventilation strategies.<sup>4</sup>

**METHODS**

All experiments were performed in accordance with the National Institutes of Health Guidelines in the Use of Laboratory Animals and approved by SUNY Upstate Medical University Institutional Animal Care and Use Committee. Male Sprague-Dawley rats (450 to 500g) were acclimatized

to the laboratory environment for 1 week before surgery. Each rat was anesthetized with a ketamine/xylazine mixture (90 mg/mL/10 mg/mL) at a dose of 0.1 mg/kg of ketamine. Animals were intubated via tracheostomy with a 2.5-mm tracheal cannula (Harvard Apparatus) and then placed on mechanical ventilation (Dräger Evita Infinity V500) with a positive end-expiratory pressure (PEEP) of 5 cm H<sub>2</sub>O and tidal volume ( $V_t$ ) of 6 mL/kg.

The rats were randomized into 1 of 3 groups: control ( $n = 2$ ), controlled mandatory ventilation (CMV;  $n = 4$ ), or airway pressure release ventilation (APRV;  $n = 4$ ). The control rats were not subjected to injury, but were briefly ventilated for 5 ventilatory cycles with  $V_t$  of 6 mL/kg, PEEP 5 cm H<sub>2</sub>O,  $F_iO_2$  0.21, and respiratory rate of 55 breaths/minute before analysis, as described in the Terminal Airway Analysis section.

**Surfactant deactivation**

In the treatment groups (CMV and APRV), surfactant deactivation was induced by intratracheal installation of 0.2% Tween-20 in normal saline (5 mL/kg), half this volume into each lung. Rats were rotated into the right and left lateral decubitus positions, respectively, for bilateral Tween distribution. Animals were then subjected to injurious mechanical ventilation with high tidal volumes ( $V_t$  16 mL/kg) and PEEP 0 cm H<sub>2</sub>O for 10 minutes before initiating respective ventilator settings.

**Controlled mandatory ventilation group**

Rats were maintained on low tidal volume ventilation ( $V_t$  6 mL/kg) with a respiratory rate of 55 breaths/minute, an I:E ratio (difference in area between inspiration and expiration) of 1:2, and  $F_iO_2$  of 0.21. They were further randomized into either PEEP 5 cm H<sub>2</sub>O (PEEP 5;  $n = 2$ ) or PEEP 16 cm H<sub>2</sub>O (PEEP 16;  $n = 2$ ). Animals were ventilated at each setting for 5 minutes to allow acclimatization and to standardize the volume history.

**Airway pressure release ventilation group**

Rats were ventilated at a plateau pressure ( $P_{High}$ ) of 35 to 40 cm H<sub>2</sub>O for a prolonged time ( $T_{High}$ ) of 1.9 to 2.0 seconds, which was set to occupy approximately 90% of the ventilatory cycle and a brief time ( $T_{Low}$ ) at the release pressure ( $P_{Low} = 0$  cm H<sub>2</sub>O). The peak expiratory flow rate (PEFR) is defined as the greatest absolute flow rate during the release from  $P_{High}$ . The flow rate at the termination of PEFR (T-PEFR) was altered by varying  $T_{Low}$  between 0.13 and 0.40 seconds so that the ratio between T-PEFR and PEFR (T-PEFR:PEFR) was 10% (APRV 10%;  $n = 2$ ) or 75% (APRV 75%;  $n = 2$ ). Animals were ventilated with  $F_iO_2$  of 0.21 at each setting for 5 minutes to allow acclimatization and to standardize the lung volume history.

### Terminal airway analysis

After ventilation with the respective settings, animals were euthanized and the lungs were excised en bloc. The lungs were held at the same airway pressure after they were excised and 1 lung was clamped and fixed in formalin at peak inspiration and the other at end expiration for histologic analysis.

The lung lobes were sectioned and sliced to 10  $\mu\text{m}$  and stained with hematoxylin-eosin. Four photomicrographs from each of the control and experimental groups at both inspiration and expiration were selected at random for analysis. Three main anatomic features were demarcated by our blinded histologist using PhotoShop CS6 (Adobe, Inc): the conducting airways (demarcated in green, defined as the airways extending from the alveolar duct proximally), the individual alveoli (lilac), and the remaining structures including interstitium, blood vessels, and lymphatics (magenta) (Fig. 1).

The representative areas and perimeters of the conducting airway and alveolar air spaces were quantitatively measured using Image-Pro Plus (MediaCybernetics).

Total air space areas were calculated as a percentage of the total frame area. Conducting airway perimeters were measured at inspiration and expiration and an average of each was taken. As previously described, micro-strain was calculated as the change in length of the conducting airway wall normalized by the original length<sup>13</sup>:

$$\text{micro-strain} = \Delta L_P / L_{Pe} \quad (\text{Equation 1})$$

where  $\Delta L_P$  is the change in perimeter length between inspiration and expiration and  $L_{Pe}$  is the original perimeter length at expiration.

In order to describe the air space relationship between the conducting airways and alveoli, we defined the ratio between the conducting airway air space area ( $C_a$ ) and alveolar area ( $A_a$ ) ( $C_a/A_a$ ).

### Statistics

Results are reported as mean  $\pm$  standard error. Continuous variables were analyzed using ANOVA. Dunnett's multiple comparison test was used for post hoc comparison of each experimental group to control. All tests were

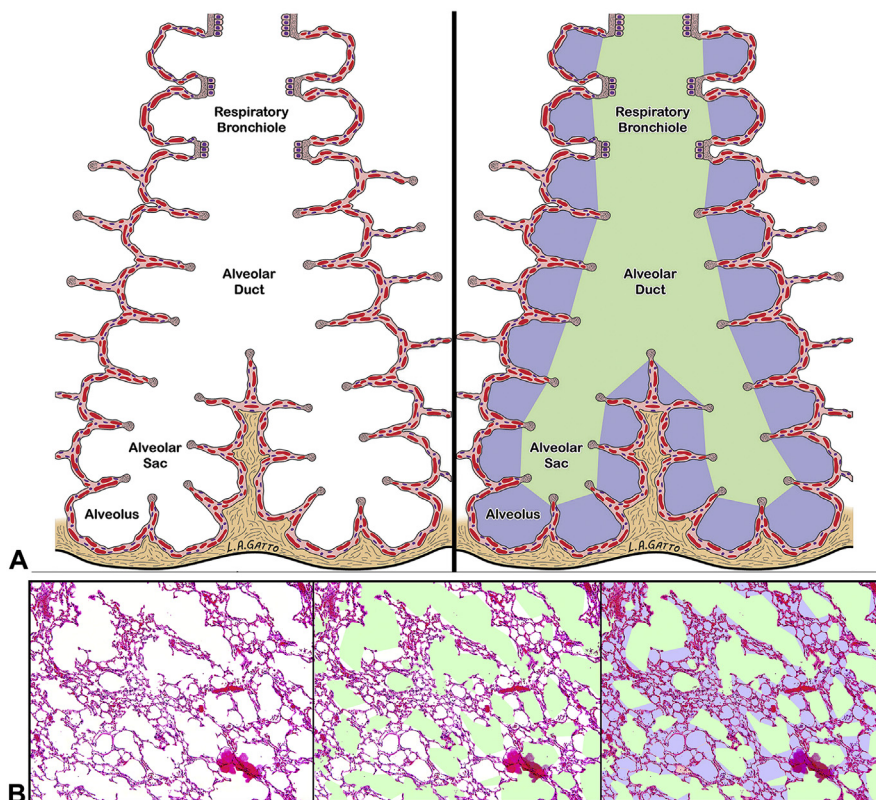


**Figure 1.** (A) Schematic of the terminal airway before and after color demarcation. (B) A standard hematoxylin-eosin staining of the lung is first analyzed for conducting airway air spaces and demarcated in green. The alveoli are demarcated in lilac while the remaining interstitium, blood vessels, and lymphatics are colored in magenta. (Histology and artwork courtesy of Louis A Gatto.)

2-tailed, and  $p$  values  $\leq 0.05$  were considered statistically significant (Prism 5.0).

## RESULTS

### Qualitative histology

In the control group, the alveoli at both inspiration and expiration appear homogeneous and relatively round, with the alveoli at expiration being slightly smaller than those at inspiration (Fig. 2). In the 4 treatment groups, the conducting airways appear to occupy more of the photomicrograph both at inspiration and expiration as compared with the control group. In particular, the conducting airways dominate the photomicrograph in APRV 10%. In PEEP 5 and APRV 10%, the alveoli appear small and heterogeneous, both at inspiration and expiration. In PEEP 16 and APRV 75%, the alveoli appear more round and homogeneous, more comparable to those in the control group. The alveoli in the APRV 75% group appear larger than the in the rest of the experimental groups, both at inspiration and at expiration.

### Terminal airway analysis

In the lungs injured by surfactant deactivation, gas was preferentially distributed to the conducting airways when compared with the control group (Table 1, Fig. 3A). However, experimental groups with higher end-expiratory pressure (ie, PEEP 16) or shorter time at expiration (ie, APRV 75%) reduced this gas redistribution to the conducting airways and improved gas distribution to the alveoli (Fig. 3A, 3B). This was evidenced by smaller conducting airway air space occupancy ( $C_a$ ) at inspiration, greater alveolar air space occupancy ( $A_a$ ) at inspiration and expiration, and a smaller ratio,  $C_a/A_a$  at inspiration (Table 1). Experimental groups with lower end expiratory pressure (ie, PEEP 5) or longer time at expiration (ie, APRV 10%) caused greater gas redistribution to the conducting airways, as supported by greater  $C_a$  as compared with  $A_a$ , measured by  $C_a/A_a$  (Table 1).

The control group had the greatest  $A_a$  at inspiration and expiration; however, this did not differ significantly from the  $A_a$  in APRV 75% (Table 1, Fig. 3B). The remaining experimental groups had significantly less  $A_a$  than control. The greatest change in  $C_a$  was in the PEEP 5 and APRV 10% group, which also had greater  $A_a$  at expiration as compared with inspiration (Fig. 3A, 3B). This was likely due to additional alveoli being “pulled into” the photomicrograph at expiration as the size of the conducting airways was reduced. This artifact precluded analysis of alveolar dynamics between inspiration and expiration, including micro-strain.

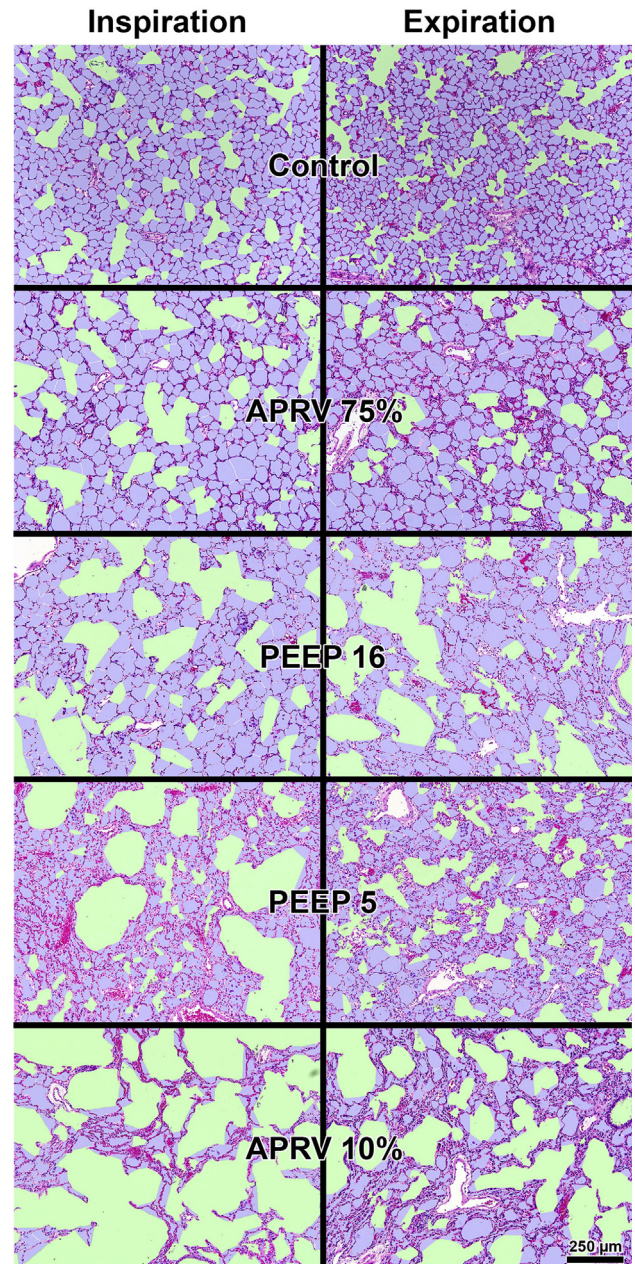


**Figure 2.** Terminal airway analysis at inspiration and expiration in control vs the 4 experimental groups. The conducting airways are depicted in green, alveoli in lilac, and remaining interstitium, blood vessels, and lymphatics in magenta.

### Airway pressure release ventilation

The APRV 75% group caused the greatest  $A_a$  at both inspiration and expiration, with values similar to control ( $p > 0.05$ ), and resulted in the least conducting airway micro-strain (Fig. 3B, Fig. 4). The APRV 10% group had the least  $A_a$  at both inspiration and expiration and the greatest conducting airway micro-strain.

**Table 1.** Relationships among Total Conducting Airway and Alveolar Area at Inspiration and Expiration and the Difference Between Inspiration and Expiration Conducting Airway Air Space Area in Controlled Mandatory Ventilation and Airway Pressure Release Ventilation

Group	Conducting airway area		I-E, %		Conducting airway perimeter		Micro-strain		C <sub>a</sub> /A <sub>a</sub>		Alveolar area	
	Ins, %	Exp, %	Ins, %	I-E, %	Ins, $\mu$ m	Exp, $\mu$ m	Ins, $\mu$ m	Exp, $\mu$ m	Ins	Exp	Ins, %	Exp, %
Control	19.0 ± 0.24	17.2 ± 0.22	1.8	324.7 ± 5.7	285.5 ± 3.45	0.137	0.33 ± 0.01	0.35 ± 0.01	57.5 ± 0.22	49.6 ± 0.25		
APRV 75%	30.5 ± 0.70*	24.6 ± 0.53 <sup>†</sup>	5.9	487.2 ± 10.9*	405.2 ± 5.9 <sup>†</sup>	0.202	0.65 ± 0.03	0.51 ± 0.01	48.7 ± 0.74	48.3 ± 0.60		
PEEP 16	33.5 ± 0.43*	30.2 ± 0.68 <sup>†</sup>	3.3	539.1 ± 11.3*	437.8 ± 10.6 <sup>†</sup>	0.231	0.81 ± 0.03	0.79 ± 0.03 <sup>†</sup>	43.8 ± 0.85*	39.7 ± 0.66 <sup>†</sup>		
PEEP 5	32.7 ± 0.57*	24.7 ± 0.53 <sup>†</sup>	8	468.5 ± 10.7*	350.7 ± 7.7	0.336	0.90 ± 0.02*	0.60 ± 0.02	37.0 ± 0.37*	41.7 ± 0.54 <sup>†</sup>		
APRV 10%	50.2 ± 0.95*	35.2 ± 0.77 <sup>†</sup>	15	655.4 ± 13.0*	470.2 ± 10.9 <sup>†</sup>	0.394	2.07 ± 0.12*	1.32 ± 0.06 <sup>†</sup>	26.5 ± 0.82*	28.7 ± 1.12 <sup>†</sup>		

Data are presented as mean ± SEM.

\*p < 0.05 vs control at inspiration.

<sup>†</sup>p < 0.05 vs control at expiration.

APRV, airway pressure release ventilation; C<sub>a</sub>/A<sub>a</sub>, conducting airway to alveolar air space area ratio; EXP, expiration; I-E, difference in area between inspiration and expiration; INS, inspiration.

### Controlled mandatory ventilation

The PEEP 16 group demonstrated greater A<sub>a</sub> than PEEP 5 at inspiration, but significantly less than control (p < 0.05) (Fig. 3B). The PEEP 16 group also had less conducting airway micro-strain than PEEP 5, but greater than APRV 75% (Fig. 4).

## DISCUSSION

Current clinical ventilator management of the lung relies on organ-level parameters even though these may not reflect the regional lung micromechanics.<sup>9,14</sup> Heterogeneous alveolar and alveolar duct compliance, which is a hallmark of lung injury, causes an abnormal distribution of strain during mechanical ventilation.<sup>15</sup> Oeckler and Hubmayr<sup>4</sup> asserted that the micro-scale distribution of stress and strain remote from the pleura remains unknown. However, understanding the mathematical relationship between the mechanical breath and the distribution of micro-scale stress and strain is a critical component in the development of optimized macro-ventilation strategies.<sup>4,9</sup> In this study, we provide a novel description of the dynamic micromechanics in the lung interior using a unique histologic technique.<sup>4</sup>

Our observations demonstrate that in the surfactant-deficient lung, air was distributed preferentially to the conducting airways rather than the alveoli. We also found that APRV 75% minimized conducting airway micro-strain and optimized alveolar occupancy (A<sub>a</sub>), as compared with the other experimental groups. Both clinical and animal studies have identified APRV 75% to be the optimal setting for lung protection.<sup>16-20</sup> Conversely, inappropriately set APRV (10%) had the greatest conducting micro-strain and least A<sub>a</sub>, suggesting that relatively minor changes in the components of the mechanical breath (~0.2 sec difference in T<sub>Low</sub>) can have a large impact on the micro-environment.

### Air space distribution

In a corollary study that used in vivo microscopy, we measured air space occupancy of the subpleural alveoli as we varied pressure and time components of the mechanical breath profile during CMV and APRV (eVideo 1, online only).<sup>9</sup> As visualized in the video, that study demonstrated that APRV 75%, with P<sub>High</sub> maintained for 90% of the breath, provided the greatest degree of alveolar air space occupancy at both inspiration and expiration. In contrast, APRV 10% with similar prolonged time at P<sub>High</sub> but a long release phase at P<sub>Low</sub> had similar A<sub>a</sub> at inspiration but demonstrated a significant reduction in alveolar occupancy at end expiration. So, this study supports our previous in vivo observations, which indicate that APRV 75% with a

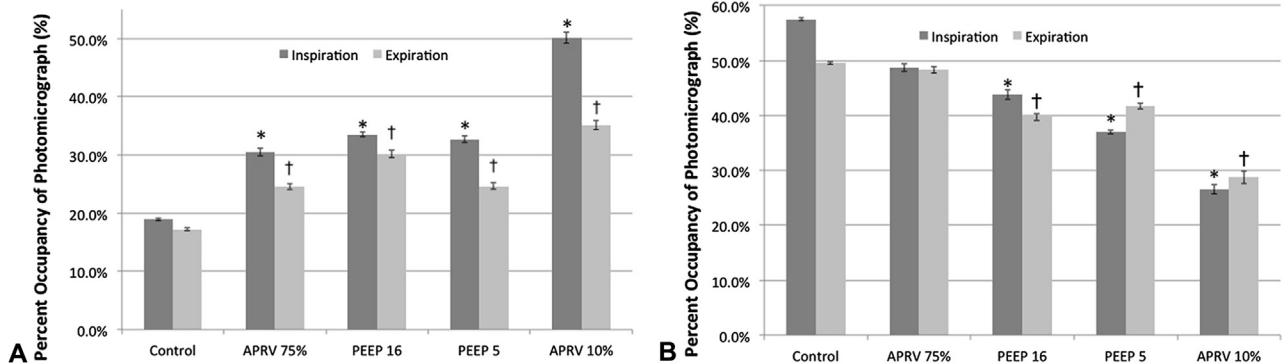


**Figure 3.** (A) Conducting airway air space occupancy at inspiration and expiration. (B) Alveolar air space occupancy at inspiration and expiration. \* $p < 0.05$  vs control at inspiration. † $p < 0.05$  vs control at expiration. APRV, airway pressure release ventilation; PEEP, positive end expiratory pressure.

prolonged time at  $T_{High}$  improves and maintains alveolar recruitment. However, unlike the subpleural alveoli in our previous investigation, this study shows that APRV 10% does not optimize alveolar occupancy in the terminal airway at inspiration. The differences in these 2 studies suggest that alveoli in the proximal lung respond differently to the mechanical breath than subpleural alveoli.

Distribution of the mechanical breath to the terminal airway has remained elusive despite decades of research. It is still unknown whether only the alveolar ducts expand during breathing while the alveoli remain relatively constant, or whether the alveoli change during tidal ventilation.<sup>21</sup> The results of this study suggest that the alveolar ducts expand and contract during tidal ventilation in the injured lung.

### Micro-strain

In the healthy lung, an intimate micromechanical relationship between the alveoli and conducting airways is maintained. This balance is disturbed in the diseased state, particularly when ventilated with settings that

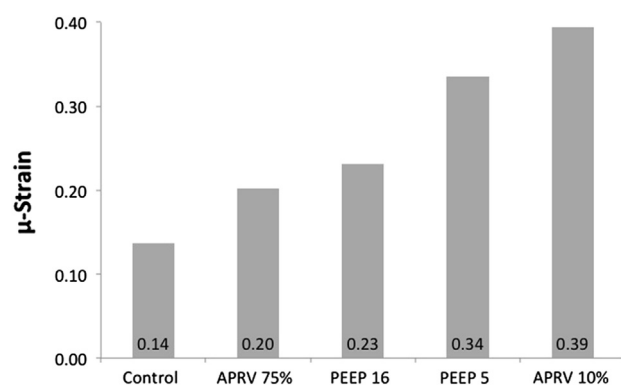


**Figure 4.** Conducting airway micro-strain ( $\mu$ -strain), calculated based on conducting airway perimeters at inspiration and expiration. APRV, airway pressure release ventilation; PEEP, positive end expiratory pressure.

have been shown harmful and associated with VILI.<sup>1</sup> It is possible that the mechanism by which inappropriate ventilator setting harms the lung is by altering the micro-strain of alveoli and connecting airways.<sup>8,9,22</sup>

Protti and associates<sup>8</sup> demonstrated that increasing degrees of whole lung dynamic strain increased the risk of developing VILI. It is also known that cyclic nonphysiologic strain injures the lung sub-units, particularly dynamic strain.<sup>23</sup> In the corollary study, we demonstrated that APRV 75% generated the smallest subpleural alveolar micro-strain and CMV with PEEP 5 the greatest (eVideo 1, online only).<sup>9</sup> In this study, however, APRV 75% demonstrated the smallest conducting airway micro-strain and APRV 10% the greatest. Taken together, these data suggest that APRV 75% reduces alveolar<sup>9</sup> and conducting airway micro-strain, both of which may be important components in preventing VILI.<sup>16-20</sup>

### Sensitivity of micromechanics to macro-ventilation settings

Airway pressure release ventilation with an appropriate release phase duration (T-PEFR:PEFR 75%) has demonstrated promising results in a retrospective data analysis of severely injured trauma patients,<sup>19</sup> a porcine sepsis and gut ischemia/reperfusion-induced ARDS model,<sup>17,18</sup> as well as in rat VILI<sup>16</sup> and hemorrhagic shock-induced ARDS models.<sup>20</sup> In this study and our previous in vivo microscopy investigation, we showed that inappropriately set APRV (ie, T-PEFR:PEFR = 10%) increases alveolar<sup>9</sup> and conducting airway micro-strain as well as preferential gas distribution away from the alveoli to the conducting airways.

In a randomized trial of 58 patients comparing APRV with synchronized intermittent mandatory ventilation, Varpula and colleagues<sup>24</sup> determined that there was no difference between APRV and synchronized intermittent mandatory ventilation in terms of clinically applicable

outcomes; however, in that study, patients on APRV had a  $T_{Low}$  set to allow the expiratory flow to decay to zero. The difference between the  $T_{Low}$  of APRV 75% ( $0.14 \pm 0.01$  seconds) and APRV 10% ( $0.34 \pm 0.02$  seconds) in this study was only 0.20 seconds. With all other breath parameters held constant, this slight difference in the  $T_{Low}$  allowed the expiratory flow to decay to nearly zero and caused marked changes in gas distribution at the terminal airway. Similarly, in a randomized prospective trial of 63 patients, Maxwell and coworkers<sup>25</sup> determined that many clinical outcomes variables were similar between APRV and low tidal volume ventilation; however, the T-PEFR:PEFR ratio was set between 25% and 75%. Although the difference in the  $T_{Low}$  between a ratio of 25% and 75% may seem insignificant, our studies have shown that the distribution of the mechanical breath to the micro-environment is markedly different.<sup>9</sup> When interpreting outcomes studies comparing any ventilator mode(s), attention to the breath settings remains of critical importance.<sup>26</sup>

### Terminal airway analysis

Several innovative techniques have been developed to investigate the terminal airway and air distribution to the lung sub-units, but very few have used these techniques to compare the impact of different ventilation strategies on the terminal airway. Many are limited by reduced resolution, inability to visualize structures deeper than the subpleural alveoli, or inability to distinguish the conducting airways from the alveoli. In general, 3-dimensional techniques offer a more complete view of the lung but are often limited by resolution or estimation by stereologic methods from serial sections in order to assess the individual acinar segments.<sup>27</sup> Standard CT images of the thorax are useful clinically, but CT does not afford the necessary resolution to be able to characterize the structure and composition of the terminal airway and therefore does not yield information regarding tissue stretch or strain.<sup>21,28</sup> Micro-CT has been used to investigate the lung microstructure and quantify alveolar surface area, density, and volume. However, the resolution decreases with increasing sample thickness and the technique has a lower resolution than standard histopathology such that very thin alveolar septae may not be visible. This suggests that histology may provide a more accurate, albeit 2-dimensional, assessment of terminal airway morphology.<sup>27,29,30</sup>

Optical coherence tomography is a high-resolution, 3-dimensional approach, which is nondestructive and may be performed such that it avoids contact with the alveolus.<sup>31</sup> Optical coherence tomography has the advantage of being able to track individual alveoli through the entire ventilator cycle, but it has a tendency to overestimate the area of alveolar walls and underestimate the alveolar

space.<sup>31</sup> Unfortunately, optical coherence tomography is limited to visualization of only the first 500  $\mu\text{m}$  of subpleural lung parenchyma; therefore, assessment of volume changes and strain in the inner lung is not feasible.<sup>31-33</sup>

In vivo microscopy has been used successfully to garner information regarding alveolar morphology in different ventilator settings.<sup>9,34</sup> But observation is limited to the immediate subpleural alveoli, and this approach requires a small opening in the chest wall and direct contact with the pleura, potentially disturbing alveolar dynamics. The use of suction to hold the tissue under the lens may cause compressive stress and deform the tissue, and the environment of the alveolus may change due to the loss of the constricting effect of the chest wall.<sup>27</sup> The loss of a volume limit and transpulmonary pressure may not adequately mimic the in vivo conditions associated with an intact chest wall.<sup>11</sup> It also does not directly visualize the inner lung and cannot characterize the space-occupying relationship between the alveoli and conducting airways.<sup>35-37</sup>

Electrical impedance tomography has also been advocated as a potential noninvasive strategy of assessing regional lung expansion. The unit of measure in this technology is the pixel, but each pixel contains several alveoli, making individual alveolar assessment difficult. Furthermore, different alveoli may be included in the same electrical impedance tomography pixel at different stages of ventilation, limiting certain dynamic measurements, including  $\mu$ -strain.<sup>38,39</sup> Electrical impedance tomography is also limited by the inability to distinguish the conducting airways from the alveoli quantitatively.

Many currently held theories on alveolar mechanics are rooted in classic histopathology studies, and this approach has remained a gold standard for the static analysis of the terminal airway.<sup>40,41</sup> This study is unique in that it allows quantification of relative air space areas as well as a comparison of lungs fixed at various points during the ventilator cycle.

### Limitations

It would not be clinically realistic to ventilate an ARDS lung with  $F_iO_2$  0.21 if the study were designed to identify pathologic changes over time caused by multiple ventilator settings. However, we believe that  $F_iO_2$  of 0.21 was appropriate for this study because it addressed how the inspired gas was accommodated by the terminal airways (ie, the alveoli and conducting airways) and did not address lung pathology. It is unlikely that a higher oxygen concentration would affect the response of the terminal airway to the mechanical breath, but the  $F_iO_2$  was standardized in both groups to ensure comparable results. Each group consisted of 2 rats, but 4 photomicrographs from each rat at each of inspiration and expiration were analyzed. At inspiration, between 3,989 and 7,550 alveoli were analyzed for a given

group, suggesting that this is still a robust analysis despite smaller group sizes. As noted previously, due to the artifact created by the large conducting airway occupancy at inspiration, alveolar micro-strain could not be reliably calculated.<sup>9</sup> Because the terminal airway analysis was performed by isolating 1 lung at inspiration and the other at expiration, a specific lung region could not be compared at both levels of inflation. In order to calculate micro-strain, the average conducting airway perimeters at inspiration and expiration were calculated, such that statistical significance could not be determined. Despite these limitations, the study provides a unique method of analyzing the terminal airway using standard histopathology techniques. To our knowledge, this is the first study to analyze the impact of various mechanical ventilation strategies on the conducting airways.

## CONCLUSIONS

In this study, we present a novel methodology to assess the impact of the mechanical breath on the terminal airway in both the injured and uninjured lung. We have shown that the gas distribution of the APRV 75% mechanical breath is more similar to the normal lung than other ventilation modes despite surfactant deactivation. Because APRV 75% improves alveolar gas delivery, conducting airway micro-strain is concurrently reduced. Our findings highlight the importance of selecting appropriate ventilation parameters so that the inspired gas reaches the alveolus. When settings are adjusted on the mechanical ventilator, consideration is not always given to how those settings affect the terminal airway. We have, therefore, also demonstrated the importance of considering the impact of the macro-ventilation settings we set with the ventilator on the micro-anatomy of the lung.

## Author Contributions

Study conception and design: Kollisch-Singule, Roy, Satalin, Ghosh, Andrews, Habashi, Nieman  
 Acquisition of data: Kollisch-Singule, Ruiz, Roy, Satalin, Snyder, Ghosh  
 Analysis and interpretation of data: Kollisch-Singule, Smith, Ruiz, Meng, Satalin, Gatto  
 Drafting of manuscript: Kollisch-Singule, Nieman  
 Critical revision: Emr, Smith, Roy, Jain, Satalin, Marx, Andrews, Habashi, Gatto

**Acknowledgment:** The authors wish to thank Dr Jason Bates for his assistance in reviewing the manuscript.

## REFERENCES

- Gajic O, Dara SI, Mendez JL, et al. Ventilator-associated lung injury in patients without acute lung injury at the onset of mechanical ventilation. *Crit Care Med* 2004;32:1817–1824.

- Bilek AM, Dee KC, Gaver DP 3rd. Mechanisms of surface-tension-induced epithelial cell damage in a model of pulmonary airway reopening. *J Appl Physiol* 2003;94:770–783.
- Kay SS, Bilek AM, Dee KC, Gaver DP 3rd. Pressure gradient, not exposure duration, determines the extent of epithelial cell damage in a model of pulmonary airway reopening. *J Applied Physiol* 2004;97:269–276.
- Oeckler RA, Hubmayr RD. Alveolar microstrain and the dark side of the lung. *Crit Care* 2007;11:177.
- Network A. Ventilation with lower tidal volumes as compared with traditional tidal volumes for acute lung injury and the acute respiratory distress syndrome. The Acute Respiratory Distress Syndrome Network. *N Engl J Med* 2000;342:1301–1308.
- Villar J, Blanco J, Anon JM, et al. The ALIEN study: incidence and outcome of acute respiratory distress syndrome in the era of lung protective ventilation. *Intensive Care Med* 2011;37:1932–1941.
- Chiumello D, Carlesso E, Cadringer P, et al. Lung stress and strain during mechanical ventilation for acute respiratory distress syndrome. *Am J Respir Crit Care Med* 2008;178:346–355.
- Protti A, Andreis DT, Monti M, et al. Lung stress and strain during mechanical ventilation: any difference between statics and dynamics? *Crit Care Med* 2013;41:1046–1051.
- Kollisch-Singule M, Emr B, Smith B, et al. Mechanical breath profile of airway pressure release ventilation: the effect on alveolar recruitment and microstrain in acute lung injury. *JAMA Surg* 2014; doi:10.1001/jamasurg.2014.1829.
- Rausch SM, Haberthur D, Stapanoni M, et al. Local strain distribution in real three-dimensional alveolar geometries. *Ann Biomed Engineer* 2011;39:2835–2843.
- Roan E, Waters CM. What do we know about mechanical strain in lung alveoli? *American Journal of Physiology. Lung Cell Molec Physiol* 2011;301:L625–635.
- Storey WF, Staub NC. Ventilation of terminal air units. *J Appl Physiol* 1962;17:391–397.
- Brewer KK, Sakai H, Alencar AM, et al. Lung and alveolar wall elastic and hysteretic behavior in rats: effects of in vivo elastase treatment. *J Appl Physiol* 2003;95:1926–1936.
- Bates JH, Davis GS, Majumdar A, et al. Linking parenchymal disease progression to changes in lung mechanical function by percolation. *Am J Respir Crit Care Med* 2007;176:617–623.
- de Ryck J, Thiesse J, Namati E, McLennan G. Stress distribution in a three dimensional, geometric alveolar sac under normal and emphysematous conditions. *Int J Chronic Obstruct Pulmonary Dis* 2007;2:81–91.
- Emr B, Gatto L, Roy S, et al. Airway pressure release ventilation prevents ventilator-induced lung injury in normal lungs. *JAMA Surg* 2013;148:1005–1012.
- Roy S, Habashi N, Sadowitz B, et al. Early airway pressure release ventilation prevents ards-a novel preventive approach to lung injury. *Shock* 2013;39:28–38.
- Roy S, Sadowitz B, Andrews P, et al. Early stabilizing alveolar ventilation prevents acute respiratory distress syndrome: a novel timing-based ventilatory intervention to avert lung injury. *J Trauma Acute Care Surg* 2012;73:391–400.
- Andrews PL, Shiber JR, Jaruga-Killeen E, et al. Early application of airway pressure release ventilation may reduce mortality in high-risk trauma patients: a systematic review of observational trauma ARDS literature. *J Trauma Acute Care Surg* 2013;75:635–641.

20. Roy SK, Emr B, Sadowitz B, et al. Preemptive application of airway pressure release ventilation prevents development of acute respiratory distress syndrome in a rat traumatic hemorrhagic shock model. *Shock* 2013;40:210–216.
21. Hubmayr RD. Perspective on lung injury and recruitment: a skeptical look at the opening and collapse story. *Am J Respir Crit Care Med* 2002;165:1647–1653.
22. Suki B, Ito S, Stamenovic D, Lutchen KR, Ingenito EP. Biomechanics of the lung parenchyma: critical roles of collagen and mechanical forces. *J Applied Physiol* 2005;98:1892–1899.
23. Gattinoni L, Protti A, Caironi P, Carlesso E. Ventilator-induced lung injury: the anatomical and physiological framework. *Crit Care Med* 2010;38:S539–548.
24. Varpula T, Valta P, Niemi R, et al. Airway pressure release ventilation as a primary ventilatory mode in acute respiratory distress syndrome. *Acta Anaesthesiologica Scandinavica* 2004;48:722–731.
25. Maxwell RA, Green JM, Waldrop J, et al. A randomized prospective trial of airway pressure release ventilation and low tidal volume ventilation in adult trauma patients with acute respiratory failure. *J Trauma* 2010;69:501–510; discussion 511.
26. Andrews PL, Scalea T, Habashi NM. What's in a name? Mechanical ventilation is at the mercy of the operator. *J Trauma Acute Care Surg* 2013;74:1377–1378.
27. Unglert CI, Namati E, Warger WC 2nd, et al. Evaluation of optical reflectance techniques for imaging of alveolar structure. *J Biomed Optics* 2012;17:071303.
28. Suki B, Sato S, Parameswaran H, et al. Emphysema and mechanical stress-induced lung remodeling. *Physiology* 2013;28:404–413.
29. Litzlbauer HD, Neuhaeuser C, Moell A, et al. Three-dimensional imaging and morphometric analysis of alveolar tissue from microfocal X-ray-computed tomography. *American Journal of Physiology. Lung Cell Molec Physiol* 2006;291:L535–545.
30. Kampschulte M, Schneider CR, Litzlbauer HD, et al. Quantitative 3D micro-CT imaging of human lung tissue. *RoFo : Fortschritte auf dem Gebiete der Rontgenstrahlen und der Nuklearmedizin* 2013;185:869–876.
31. Meissner S, Knels L, Schnabel C, et al. Three-dimensional Fourier domain optical coherence tomography in vivo imaging of alveolar tissue in the intact thorax using the parietal pleura as a window. *J Biomed Optics* 2010;15:016030.
32. Popp A, Wendel M, Knels L, et al. Imaging of the three-dimensional alveolar structure and the alveolar mechanics of a ventilated and perfused isolated rabbit lung with Fourier domain optical coherence tomography. *J Biomed Optics* 2006;11:014015.
33. Namati E, Thiesse J, de Ryk J, McLennan G. Alveolar dynamics during respiration: are the pores of Kohn a pathway to recruitment? *Am J Respiratory Cell Molec Biol* 2008;38:572–578.
34. Pavone LA, Albert S, Carney D, et al. Injurious mechanical ventilation in the normal lung causes a progressive pathologic change in dynamic alveolar mechanics. *Crit Care Med* 2007;11:R64.
35. DiRocco JD, Pavone LA, Carney DE, et al. Dynamic alveolar mechanics in four models of lung injury. *Intensive Care Med* 2006;32:140–148.
36. Carney D, DiRocco J, Nieman G. Dynamic alveolar mechanics and ventilator-induced lung injury. *Crit Care Med* 2005;33:S122–128.
37. Halter JM, Steinberg JM, Gatto LA, et al. Effect of positive end-expiratory pressure and tidal volume on lung injury induced by alveolar instability. *Crit Care* 2007;11:R20.
38. Muders T, Luepschen H, Zinserling J, et al. Tidal recruitment assessed by electrical impedance tomography and computed tomography in a porcine model of lung injury\*. *Crit Care Med* 2012;40:903–911.
39. Bikker IG, Leonhardt S, Reis Miranda D, et al. Bedside measurement of changes in lung impedance to monitor alveolar ventilation in dependent and non-dependent parts by electrical impedance tomography during a positive end-expiratory pressure trial in mechanically ventilated intensive care unit patients. *Crit Care* 2010;14:R100.
40. Wilson TA, Bachofen H. A model for mechanical structure of the alveolar duct. *J Applied Physiol* 1982;52:1064–1070.
41. Bachofen H, Gehr P, Weibel ER. Alterations of mechanical properties and morphology in excised rabbit lungs rinsed with a detergent. *J Applied Physiol* 1979;47:1002–1010.